Lattice Thermal Conductivity of GaAs

M. Ataullah Ansari[a], V. Ashokan[b], B.D. Indu[b,*] and R. Kumar[c]

[a]Physics Department, Techwords W.G.V.S. Group of Institution, Manglour, Roorkee, 247 667, Uttarakhand, India

[b]Department of Physics, Indian Institute of Technology, Roorkee, 247667, Uttarakhand, India

[c]Physics Department, Gurukul Kangri Vishvavidyalaya, Haridwar, 249 404, Uttarakhand, India

(Received June 23, 2011)

A new approach to evaluate the relaxation times of various collision events responsible for thermal transport has been reported through which various deficiencies of earlier models of lattice thermal conductivity have been resolved. These investigations involve the evaluation of the phonon Green functions via a non-perturbative approach. The new expressions of relaxation times expressions for scattering of phonons by boundaries, atomic impurities, phonon–phonon scattering, electron–phonon scattering are the new features of the theory. The lattice thermal conductivity of three samples of GaAs has been analyzed on the basis of modified Callaway model and fairly good agreement between theory and experimental observations has been reported.

PACS: 63.20.kd, 66.70.Df, 63.22.Rc, 63.20.Ry

1. Introduction

The anharmonicities of lattice forces which are also responsible for thermal expansion govern the heat transport by lattice waves in solids along with various imperfections and the external boundaries of crystals. Thermal conductivity has been commonly used as fundamental transport property which successfully characterizes the broad range of crystalline solids and is physically important in understanding the acoustical behavior of low dimensional systems nowadays. It was enumerated in literature [1, 2] that the theory of lattice thermal conductivity (LTC) based on the Boltzmann transport equation approach via relaxation time approximation [3–5] suffer from the usual shortcomings of kinetic theory. The phonon transport theory acquired a more rigorous basis with the use of energy flux correlation techniques [1, 6–8], but these theories could not probe into successful numerical estimates. Callaway [9] presented a very successful, more amenable to calculations and widely accepted but simple phenomenological model of LTC in the form

$$\kappa = \frac{k_{\mathrm{B}}(\beta\hbar)^2}{2\pi^2 v}\int_0^{\omega_{\mathrm{D}}} \tau(\omega)\,\omega^4\,\mathrm{e}^{\beta\hbar\omega}(\mathrm{e}^{\beta\hbar\omega}-1)^{-2}\,\mathrm{d}\omega, \quad (1)$$

where $\tau(\omega)$ is the total relaxation time for all scattering processes. In his model Callaway has however, assumed (i) the Debye spectrum for phonons which allows neglecting the anisotropy and dispersion effects, (ii) no distinction between phonon polarization (single mode relaxation time), and (iii) additivity of frequency dependent phonon relaxation times (frequent use of Matthiessen's rule). If one considers the scattering processes as independent, the scattering probabilities may be taken as additive so that

$$\tau^{-1}(\omega) = \sum_i \tau_i^{-1}(\omega), \quad (2)$$

where $\tau_i(\omega)$ represents the relaxation time for a single scattering process and is normally obtained by perturbation techniques. The assumptions made by Callaway decisively entered some inadequacies in his LTC expression and Erdos and Haley [10] for the first time critically reviewed them with some justifications. The objections appearing due to the assumption of no distinction between phonon polarizations was for the first time removed by Holland [11] with the help of two-mode analysis. In his work, Holland extended the Callaway model by considering the separate contributions of longitudinal acoustic and transverse acoustic phonons including some dispersion and using different forms of relaxation times. This theory has been further refined by several authors [12–15] to analyze the lattice thermal conductivity of several samples with the help of better dispersion and relaxation times and obtained excellent fits. In the Sharma–Dubey–Verma (SDV) [14] and Tiwari–Agrawal (TA) [15] models improved attempts have been made to involve the contribution of phonon dispersion. The work of several authors [16–25] has made significant contributions with newer concepts to improve and repair the original Callaway's phenomenological model and really opened new windows in the field. In the mean time it is noteworthy to comment that some authors [26–29] have made significant contribution to the theory of LTC based on variational and many body approaches. However, the adequate justification to some questions remained unattempted. The comments and investigations on the additivity of relaxation time were further made by Altukov and Zavt [30] but the successful attempts to resolve this

* corresponding author; e-mail: drbdindu@gmail.com

difficulty were made by Gairola [31] and Bahuguna et al. [32] with sound justifications. The low temperature region of lattice thermal conductivity curve till maximum is of extreme importance in the analytical study of experimental data where a large number of scattering processes impart to the thermal transport, which comes into play via Callaway's model. The work of Boriodo et al. [33–36] added a feature to the theory of LTC from first principles approach in which they have presented a method to describe LTC free of adjustable parameters.

In the present paper the new approach [31, 32] has been utilized to analyze the lattice thermal conductivity of GaAs samples with some additional findings and an excellent agreement between theory and experimental data has been reported in the following sections.

2. Theory

In order to investigate the quantum dynamics of the system and to explore the underlying microscopic mechanism of thermal transport, we consider the Hamiltonian of the second quantized form as

$$H = H_{\mathrm{e}} + H_{\mathrm{p}} + H_{\mathrm{ep}} + H_{\mathrm{A}} + H_{\mathrm{D}}, \tag{3}$$

where H_{e}, H_{p}, H_{ep}, H_{A} and H_{D} stand for unperturbed electron Hamiltonian, harmonic phonon Hamiltonian, electron–phonon Hamiltonian, anharmonic Hamiltonian up to quartic order and defect Hamiltonian, respectively, and can be expressed as [37–40]:

$$H_{\mathrm{e}} = \sum_{q} \hbar\omega_q b_q^* b_q, \tag{4a}$$

$$H_{\mathrm{p}} = \sum_{k} \frac{\hbar\omega_k}{4}(A_k^* A_k + B_k^* B_k), \tag{4b}$$

$$H_{\mathrm{ep}} = \sum_{q,k,\sigma} \left(g_k b_{\mathrm{Q}\sigma}^* b_{q\sigma}\right) B_k, \tag{4c}$$

$$H_{\mathrm{A}} = \sum_{s\geq 3} \sum_{k_1 \ldots k_s} \hbar V_s(k_1, k_2 \ldots k_s) A_{k_1} A_{k_2} \ldots A_{k_s}, \tag{4d}$$

$$H_{\mathrm{D}} = \sum_{k_1,k_2} \hbar[-C(k_1,k_2) B_{k_1} B_{k_2} + D(k_1,k_2) A_{k_1} A_{k_2}]. \tag{4e}$$

The operators $A_k = a_k + a_{-k}^* = A_{-k}^*$ and $B_k = a_k - a_{-k}^* = -B_{-k}^*$ represent the phonon field and momentum operator, they satisfy the commutation relation,

$$[B_k, A_{k'}] = 2\delta_{k-k'}, \tag{5}$$

$$[A_k, A_{k'}] = [B_k, B_{k'}] = 0. \tag{6}$$

In the above equations, a_k (a_k^*) and $b_{q\sigma}$ ($b_{q\sigma}^*$) are the phonon and electron annihilation (creation) operator with phonon wave vector k (for brevity we have taken $k \equiv kj$, j being polarization index) and electron wave vector q, respectively (σ stands for spin ($\uparrow$ or $\downarrow$) and g_k is the electron–phonon coupling constant). The coefficients $C(k_1,k_2)$ and $D(k_1,k_2)$ depend upon change in mass and force constant, due to substitutional impurity, respectively and given by [8, 40, 41]:

$$C(k_1,k_2) = \left(\frac{M_0}{4N\mu}\right)(\omega_{k_1}\omega_{k_2})^{1/2}[e(k_1)e(k_2)] \times \left[\sum_{l}^{N} c\,\mathrm{e}^{\mathrm{i}(k_1+k_2)R_l} - \sum_{i}^{n} \mathrm{e}^{\mathrm{i}(k_1+k_2)R_i}\right], \tag{7}$$

$$D(k_1,k_2) = (4N)^{-1}(\omega_{k_1}\omega_{k_2})^{-1/2} \times \sum_{l,l'}\left(\frac{\phi_{l,l'}}{M_0}\right)[e(k_1)e(k_2)]\,\mathrm{e}^{\mathrm{i}(k_1 R_l + k_2 R_l')}, \tag{8}$$

where $c = n/N$ and $\mu = MM'/(M'-M)$. Here $M_0^{-1} = c/M' + (1-c)/M$ is the effective atomic mass as seen by the phonon in the crystal, R_l label the equilibrium position of the l-th atom in the crystal, the symbol i designates the position of impurity atom, $e(k)$ is the polarization vector and $\phi_{l,l'}$ represents the change in the harmonic force constant due to defects. For convenience, we have used index k to denote kj, where k is the phonon wave vector and j labels the branch of the frequency spectrum. The anharmonicity coefficients $V_s(k_1, k_2 \ldots k_s)$ are the Fourier transform of s-th order anharmonic force constant and are symmetric with respect to the pair of lattice vibration indices k_s:

$$V_3(\boldsymbol{k}_1,\boldsymbol{k}_2,\boldsymbol{k}_3) = \frac{1}{3!}\left(\frac{\hbar}{8N}\right)^{1/2} \frac{\Delta(\boldsymbol{k}_1,\boldsymbol{k}_2,\boldsymbol{k}_3)\phi_3(\boldsymbol{k}_1,\boldsymbol{k}_2,\boldsymbol{k}_3)}{(\omega_{\boldsymbol{k}_1}\omega_{\boldsymbol{k}_2}\omega_{\boldsymbol{k}_3})^{1/2}},$$

$$\phi_3(\boldsymbol{k}_1,\boldsymbol{k}_2,\boldsymbol{k}_3) = \frac{1}{M^{3/2}}{\sum_{l,l'}}' \sum_{x_1,x_2,x_3} \phi^{(3)}_{x_1,x_2,x_3}(l,l') \times e(\boldsymbol{k}_1)e(\boldsymbol{k}_2)e(\boldsymbol{k}_3)\,\mathrm{e}^{2\pi\,\mathrm{i}(\boldsymbol{k}_1,\boldsymbol{k}_2,\boldsymbol{k}_3)\cdot r_0(l,l')} \tag{9}$$

and

$$V_4(\boldsymbol{k}_1,\boldsymbol{k}_2,\boldsymbol{k}_3,\boldsymbol{k}_4) = \frac{\hbar}{4!(4N)} \frac{\Delta(\boldsymbol{k}_1,\boldsymbol{k}_2,\boldsymbol{k}_3,\boldsymbol{k}_4)\phi_4(\boldsymbol{k}_1,\boldsymbol{k}_2,\boldsymbol{k}_3,\boldsymbol{k}_4)}{(\omega_{\boldsymbol{k}_1}\omega_{\boldsymbol{k}_2}\omega_{\boldsymbol{k}_3}\omega_{\boldsymbol{k}_4})^{1/2}},$$

$$\phi_4(\boldsymbol{k}_1,\boldsymbol{k}_2,\boldsymbol{k}_3,\boldsymbol{k}_4) = \frac{1}{M^2}{\sum_{l,l'}}' \sum_{x_1,x_2,x_3,x_4} \phi^{(4)}_{x_1,x_2,x_3,x_4}(l,l') \times e(\boldsymbol{k}_1)e(\boldsymbol{k}_2)e(\boldsymbol{k}_3)e(\boldsymbol{k}_4)\,\mathrm{e}^{2\pi\,\mathrm{i}(\boldsymbol{k}_1,\boldsymbol{k}_2,\boldsymbol{k}_3,\boldsymbol{k}_4)r_0(l,l')}, \tag{10}$$

where

$$\Delta\boldsymbol{k} = \begin{cases} 1 & \text{if } \boldsymbol{k} = 0 \text{ or a reciprocal lattice vector,} \\ 0 & \text{otherwise.} \end{cases} \tag{11}$$

In the above expression $e(\boldsymbol{k}_i)$ are the eigenvectors and the prime over summation states that the exclusion of the terms with $l = l'$ and $\phi^{(s)}_{x_1,x_2,\ldots x_s}(l,l')$ are the expansion coefficients [42].

In order to obtained the line shape of phonon spectrum let us consider the evaluation of the double time temperature dependent retarded Green function

$$G_{k,k'}(t-t') = \langle\langle A_k(t); A_{k'}^*(t')\rangle\rangle = -\mathrm{i}\,\theta(t-t')\langle[A_k(t), A_{k'}^*(t')]\rangle \tag{12}$$

via Hamiltonian (3) with the help of quantum dynamical equation of motion technique and Dyson's equation ap-

proach which results in the following form:

$$G_{k,k'}(\omega) = \frac{\omega_k \eta_{k,k'}}{\pi\left[\omega^2 - \tilde{\omega}_k^2 - 2\omega_k \tilde{P}(k,k',\omega)\right]}, \tag{13}$$

where $\tilde{\omega}_k$ is the renormalized phonon frequency and $\tilde{P}(k,k',\omega)$ is the self-energy operator or response function,

$$\tilde{P}(k,k',\omega + \mathrm{i}\epsilon) = \lim_{\epsilon \to 0^+} \Delta_k(\omega) - \mathrm{i}\Gamma_k(\omega), \tag{14}$$

where $\Delta_k(\omega)$ is the shift in the phonon frequency of the perturbed mode and is the real part of $\tilde{P}(k,k',\omega)$ and the imaginary part $\Gamma_k(\omega)$ is the phonon frequency linewidth at the half maximum of the phonon frequency peak. In the new approach (quantum dynamical many body theory) of line widths, the relaxation times for various scattering processes can be expressed as [31, 32]:

$$\tau^{-1}(\omega) = \Gamma_k(\omega), \tag{15}$$

where the phonon frequency line width of different contribution is given by

$$\tau^{-1}(\omega) = \Gamma_k^{\mathrm{D}}(\omega) + \Gamma_k^{\mathrm{3A}}(\omega) + \Gamma_k^{\mathrm{4A}}(\omega) + \Gamma_k^{\mathrm{AD}}(\omega) + \Gamma_k^{\mathrm{ep}}(\omega) + \tau_{\mathrm{CB}}^{-1} + \tau_R^{-1}(\omega). \tag{16}$$

In above equation various superscripts D, A, 3A, 4A, AD and ep stand for the contribution coming from defect scattering, anharmonic (cubic 3A and quartic 4A) phonon scattering, anharmonic–defect interference scattering and electron–phonon scattering. τ_{CB}^{-1} and $\tau_R^{-1}(\omega)$ describes the combined boundary and resonance scattering relaxation times, respectively. A brief account of these quantities is broadly described as follows.

2.1. Combined boundary scattering

At very low temperatures the first and the foremost scattering phenomenon which dominantly contributes to the thermal conductivity is the combined boundary scattering which can be described by [43, 44]:

$$\tau_{\mathrm{CB}}^{-1} = v/L(B), \tag{17}$$

where $L(B)^{-1} = \frac{1}{2v}(t_1^{-1} + t_2^{-1})$, $B_{\mathrm{I}} = 1.7858 t^{-1}(t_1^{-1} + t_2^{-1})^{-1}$ is the internal boundary parameter which is related to large scale fluctuations in the crystal micro boundaries, where t is the time taken to traverse the path l in the absence of internal boundaries. The phonon is traversing the free path in time t_1 with average phonon velocity v before scattering from the microboundary. After scattering, it will not traverse exactly the same path in reverse direction, but it may be assumed that the phonon apparently reaches the previous position after time t_2 to repeat scattering. Hence, $L(B)$ is different from the Casimir length L and will offer higher thermal resistance than L and the conductivity curve falls off more rapidly as shown in Fig. 1.

2.2. Point defect scattering

At very low temperatures below the conductivity maximum the scattering due to isotopic point impurities etc.

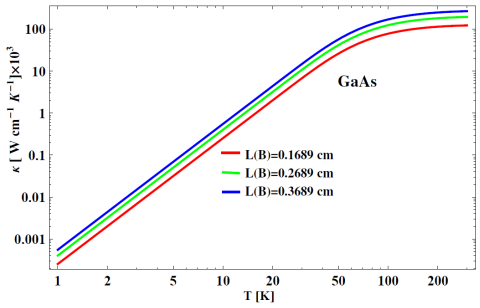

Fig. 1. Effect of combined boundary scattering length on LTC.

emerges from the next dominant collision processes and has been described by Klemens [3, 13] as

$$\tau_{\mathrm{D}}^{-1}(\omega) = A\omega^4, \tag{18}$$

where $A = \frac{\nu_0 \Gamma}{4\pi\nu^3}$ and $\Gamma = \sum_i f_i\left(1 - \frac{m_i}{\bar{m}}\right)^2$. Similar results for the impurity scattering relaxation time can be obtained from $\Gamma_k^{\mathrm{D}}(\omega)$ after some algebraic simplification in the following form [40, 45]:

$$\Gamma_k^{\mathrm{D}}(\omega) = 8\pi\epsilon(\omega) \sum_{k_1} R(-k,k_1)R^*(-k,k_1) \times \omega_{k_1}\delta\left(\omega^2 - \tilde{\omega}_{k_1}^2\right) \approx A_1\omega^4 + A_2\omega^2 \tag{19}$$

with

$$R(k_1,k_2) = (\omega_{k_2}/\omega_{k_1})C(k_1,k_2) + D(k_1,k_2) + 4\sum_{k_2'} C(-k_1,k_2')D(-k_2',k_2)\omega_k^{-1} \tag{20}$$

and

$$\epsilon(\omega) = \begin{cases} 1 & \text{for } \omega > 0, \\ -1 & \text{for } \omega < 0. \end{cases} \tag{21}$$

The coefficients A_1 and A_2, respectively, describe the mass and force constant changes occurring as a result of the presence of isotopic defects in the host crystal and can be readily obtained from Eq. (19). The contribution of force constant changes due to substitutional point defects is the new addition in the Klemens [3, 13] theory of LTC and its importance will be discussed in the section describing analysis of LTC. However, the effects of mass and force constant changes are depicted in Figs. 2 and 3.

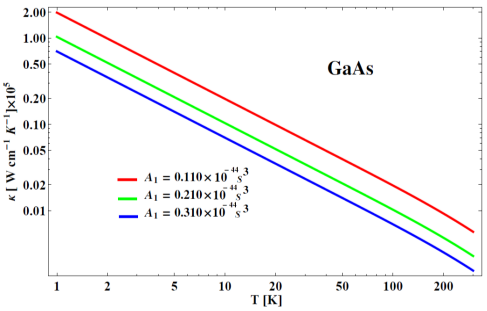

Fig. 2. Variation of LTC at different impurity concentrations.

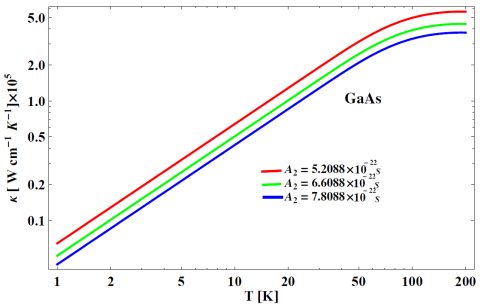

Fig. 3. Effect of force constant changes on LTC of GaAs (sample III).

2.3. Phonon–phonon scattering

As the temperature rises towards conductivity maximum more and more phonons get excited and thus the three-phonon processes are invoked and appear as the dominant scatterers. These processes have been described in the form [4, 14, 46]:

$$\tau_{\rm ph}^{-1} = \begin{cases} B\omega^2T^3 & \text{at low } T, \\ B'\omega^2T^2 & \text{at high } T. \end{cases} \tag{22}$$

The ω and T dependences of $\tau_{\rm ph}^{-1}$ have been freely varied without any appropriate justification by a large number of authors [4, 11, 12, 14, 15, 47]. The work of several authors [4, 11, 12, 47] on phonon–phonon processes (effective around LTC maximum) and the investigations by Pomeranchuk [48, 49] on four-phonon processes (significant at high temperatures) are worth mentioning. The use of frequency line width enables to fix the problem via the following expressions [40, 45] for three- and four-phonon processes:

$$\begin{aligned} \Gamma_k^{\rm 3A}(\omega) &= 18\pi\epsilon(\omega) \sum_{k_1,k_2} |V_3(k_1,k_2,-k)|^2 \\ &\times \eta_1\left[S_{+\alpha}\omega_{+\alpha}\delta(\omega^2-\omega_{+\alpha}^2) + S_{-\alpha}\omega_{-\alpha}\delta(\omega^2-\omega_{-\alpha}^2)\right] \\ &\approx \lambda V\omega_k^2\theta(\omega_L-\omega_k)/16\pi N\beta\hbar a_0 v_p^2 \approx B\omega^2T, \end{aligned} \tag{23}$$

$$\begin{aligned} \Gamma_k^{\rm 4A}(\omega) &= 48\pi\epsilon(\omega) \sum_{k_1,k_2,k_3} |V_4(k_1,k_2,k_3,-k)|^2 \\ &\times \eta_2\left[S_{+\beta}\omega_{+\beta}\delta(\omega^2-\omega_{+\beta}^2) + 3S_{-\beta}\omega_{-\beta}\delta(\omega^2-\omega_{-\beta}^2)\right] \\ &\approx (\hbar/48M)(a_0\hbar\eta\phi^{IV}V/4\pi^2\beta\phi^{II}\nu^3)^2 \\ &\times (\tilde\omega_k^2+\tilde\omega_{k_1}^2-\tilde\omega_{k+k_1}^2) \approx B_{\rm H}\omega^2T^2, \end{aligned} \tag{24}$$

where λ is the dimensionless quantity and $\omega_k = \omega_L\sin(\pi k a_0)$ which shows the exact frequency and temperature dependence. The various symbols appearing in the above equations are obtainable in the form [40]:

$$S_{\pm\alpha} = n_{k_2} \pm n_{k_1}, \tag{25}$$

$$S_{\pm\beta} = 1 \pm n_{k_1}n_{k_2} \pm n_{k_2}n_{k_3} \pm n_{k_3}n_{k_1}, \tag{26}$$

$$\omega_{\pm\alpha} = \tilde\omega_{k_1} \pm \tilde\omega_{k_2}; \quad \omega_{\pm\beta} = \tilde\omega_{k_1} \pm \tilde\omega_{k_2} \pm \tilde\omega_{k_3}, \tag{27}$$

$$\eta_{i-1} = \frac{\omega_{k_1}\omega_{k_2}\ldots\omega_{k_i}}{\tilde\omega_{k_1}\tilde\omega_{k_2}\ldots\tilde\omega_{k_i}}; \quad n_k = \frac{\tilde\omega_k}{\omega_k}\coth\frac{\beta\hbar\tilde\omega_k}{2}. \tag{28}$$

Obviously, as described in Eqs. (23) and (24), B and $B_{\rm H}$ along with mass and crystal volume chiefly depend on the cubic and quartic force constants. At conductivity maximum umklapp processes contribute more effectively as compared to normal processes. However, Callaway [9, 29] has taken the relaxation time for normal three-phonon processes and for umklapp processes proportional to $(\omega^2T^3)^{-1}$ and $(e^{\theta/aT}\omega^2T^3)^{-1}$, respectively. The four-phonon processes contribute at high temperatures and are not considered in the present case. The role of three- and four-phonon processes in semiconductors has been reanalyzed by Boriodo et al. [33–36] with the help of an *ab initio* approach.

2.4. Interference scattering

The phonons present in the anharmonic fields (cubic and/or quartic) start interacting with the phonons of localized fields and give rise to impurity anharmonic interaction modes (interference modes). These modes give rise to the interference scattering of phonons due to simultaneous involvement of localized and anharmonic fields. This scattering dominates near and above of thermal conductivity maximum where conventional impurity scattering starts losing its influence. The phonon line width for this scattering is given by [40]:

$$\begin{aligned} \Gamma_k^{\rm 3D}(\omega) &= 16\sum_{k_1}|C(-k,k_1)|^2\omega_k^{-2}(\Gamma_k^{\rm 3A}(\omega))_{k\to k_1} \\ &\approx (3\lambda V\mu_{-2}/\pi\beta\hbar a_0)\left[(M_0^2c(1-c)/4N\mu V)^2\right]\omega_k^4 \\ &\approx D\omega^4T. \end{aligned} \tag{29}$$

Here μ_{-2} is the second negative moment and c is the impurity concentration. The processes like $\Gamma_k^{\rm 4D}(\omega)$ contribute at high temperatures and are not discussed here. The effect of interference scattering events ($\Gamma_k^{\rm 3D}(\omega)$ only) has been shown in Fig. 4.

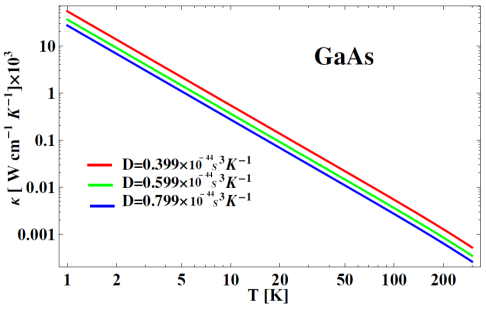

Fig. 4. Influence of interference scattering on LTC.

2.5. Electron–phonon scattering

The possibility of electrons carrying heat as well as acting as scatterers was entertained by Ziman [50] considering the parabolic bands and derived the relaxation time in the form

$$\tau_{\rm ep}^{-1} = DT\ln\left(\frac{1+\exp(\eta^* - N/T - PTx^2 + x/2)}{1+\exp(\eta^* - N/T - PTx^2 - x/2)}\right), \tag{30}$$

where $x = \frac{\hbar\omega}{k_B T}$, $D = \frac{\chi^2 m_d^{*2} k_B}{4\pi\hbar^4 \varrho v_l}$, $N = \frac{m_d^* v_l^2}{2k_B}$, $P = \frac{k_B}{8m_d^* v_l^2}$. Here χ, m_d^*, ϱ, v_l and η^* are deformation potential, density of states effective mass, density of the crystal, longitudinal phonon velocity, and reduced Fermi energy, respectively. Based on this formalism sufficient attempts were made to understand the role of electron–phonon collision events [5, 20, 51].

In order to understand the phenomenon of electron–phonon scattering with the help of present approach we use the similar quantum dynamical approach (dealt in preceding sections) to obtain the electron Green function

$$G_{q,q'}(t-t') = \langle\langle b_q^*(t); b_{q'}(t')\rangle\rangle = -\mathrm{i}\theta(t-t')\langle\big[b_q^*(t), b_{q'}(t')\big]\rangle \tag{31}$$

via Hamiltonian (3) in the form

$$G_{q,q'}(\omega) = \frac{4\omega_q \delta_{qq'}}{2\pi\big[\omega^2 - \bar{\omega}_q^2 + \mathrm{i}4\omega_q \Gamma_q(\omega)\big]}. \tag{32}$$

After some algebra the line width for electron–phonon collision processes can be described in the form [52–54]:

$$\Gamma_{\mathrm{eph}}(\omega) = x^2 T^2 \Big[A_{e_1} \coth(3x/2) - A_{e_2}(\mathrm{e}^{x/2}+1)^{-1}\Big], \tag{33}$$

where A_{e_1} and A_{e_2} are constants which depend on material characteristics and electron–phonon coupling constant g_k. This term is very sensitive because the negative term changes the scenario according to the values of A_{e_1} and A_{e_2} and its utmost effect in superconductors [54]. The variation of $\Gamma_{\mathrm{eph}}(x) = \tau_{\mathrm{eph}}^{-1}$ with x and T is shown in Fig. 5 with $A_{e_1} = 0.4895 \times 10^3$ K^{-2} s^{-1} and $A_{e_2} = 1.4685 \times 10^3$ K^{-2} s^{-1}, which clearly exhibits that electron–phonon scattering lifetime is a highly sensitive quantity and acquires both negative and positive values. In the inset the variation of $\Gamma_{\mathrm{eph}}(x)$ with temperature shows that for higher values of x its value rises with T.

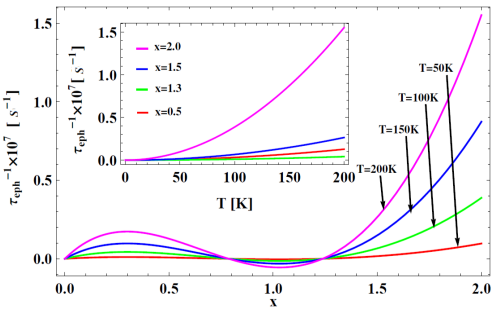

Fig. 5. Variation of τ_{eph}^{-1} versus x (in inset τ_{eph}^{-1} versus T).

The behaviour of electron–phonon line width $\Gamma_{\mathrm{eph}}(x)$ on LTC is depicted in Fig. 6 when both reduced frequency x and temperature T are simultaneously varied.

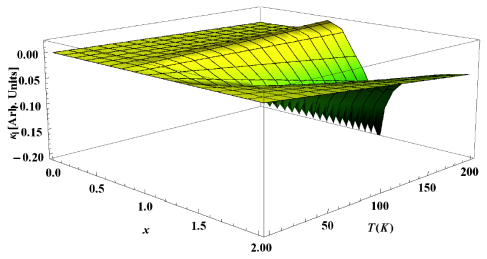

Fig. 6. Influence of electron–phonon line width on LTC.

2.6. Resonance scattering

The results of Pohl and Walker [55, 56] on resonance scattering mechanisms indicate that the dips present in the LTC curve at temperatures just above the maximum in κ are also associated with impurities. In fact if one examines the older data on Si [47] a similar dip can be noticed. It was only when the oxygen was removed from the Si that the dip disappeared from the data and the isotope scattering could be used to obtain a good fit. Data which can be characterized as having a bump or dip can often be fitted by using a resonance-type relaxation time of the form first used by Pohl [55, 57] which is given by

$$\tau_R^{-1}(\omega) = \frac{R\omega^2 T^n}{(\omega_0^2 - \omega^2)^2 + (\Omega/\pi)^2 \omega_0^2 \omega^2}, \tag{34}$$

where R is a proportionality constant containing the concentration of impurities causing the resonance scattering, ω_0 is the resonance frequency, and Ω describes damping of the resonance. For GaAs sample use of (34) with $n = 0$ can be obtained by considering inelastic scattering of phonons by localized modes, in which the impurity centers are polyatomic [58]. Figure 7 depicts that the influence of resonance scattering only on LTC other collision events has been overlooked.

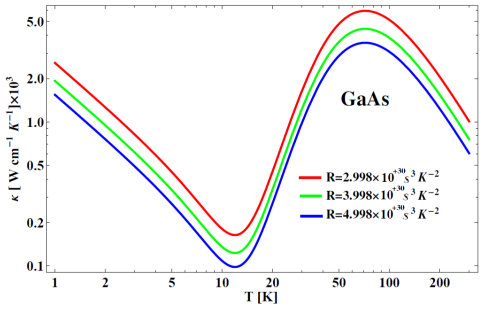

Fig. 7. Influence of resonance scattering on LTC.

3. Analysis of thermal conductivity

GaAs (III–V compound) the direct band gap semiconductor with band gap 1.42 eV has the crystal structure (zinc blende) composed of two sublattices, each face centered cubic (fcc) and offset with respect to each other by

half the diagonal of the fcc cube. Semi-insulating GaAs is a semiconductor quality material which meets some important requirements, namely: (i) lowest possible density of crystalline defects, such as dislocations, stacking faults, and precipitates. (ii) Absence of undesirable substrate active layer interface effects, e.g., light sensitivity and back-gating. (iii) Thermally stable during epitaxial growth or anneal of ion-implanted active layer. (iv) The active layer properties by out diffusion of impurities from substrate during thermal processing are not degraded. Experimental observations reveal that the thermal conductivity of such pure single crystal semiconductors is zero at 0 K and rises approximately exponentially up to a maximum value near 10 K (according to Grimvall [29] the maximum crudely lies just below $T = 0.1\theta_{\rm D}$) and falls off somewhat faster than T^{-1} and in the rest temperature range approximately varies as T^{-1} at higher temperatures [28, 29, 59].

TABLE

Constants and parameters used in the analysis of thermal conductivity of GaAs.

Samples	$L(B)$ [cm]	$\theta_{\rm D}$ [K]	A_1 [$s^3\times10^{-44}$]	A_2 [$s\times10^{-23}$]	B [$s\,K^{-1}\times10^{-23}$]	D [$s^3\,K^{-1}\times10^{-44}$]	v [$cm\,s^{-1}\times10^5$]	R [$s^3\,K^{-2}\times10^{30}$]	Ω [$s^{-1}\times10^2$]	ω_0 [$s^{-1}\times10^{12}$]
I	0.1689	345	0.110	–	68.09911	0.399	3.3	2.998	0.010	6.91822
II	0.1292	345	0.2643	52.0882	152.050	0.5652	3.3	1.011	0.99	5.99015
III	0.053	345	6.990	2.6735	20.370	0.59484	3.3	–	–	–

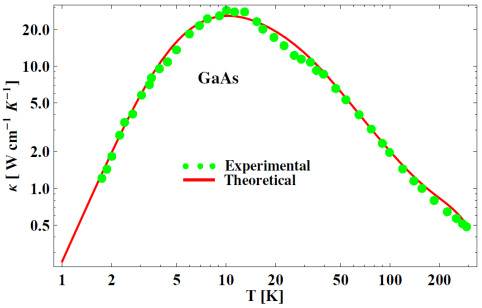

Fig. 8. Analysis of thermal conductivity of GaAs (sample I).

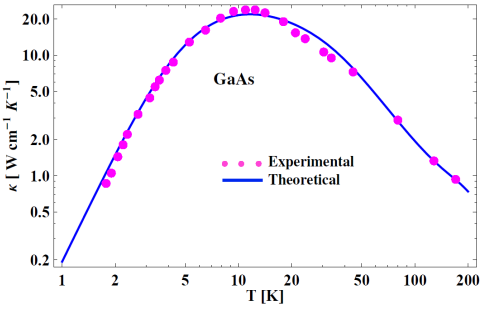

Fig. 9. Analysis of thermal conductivity of GaAs (sample II).

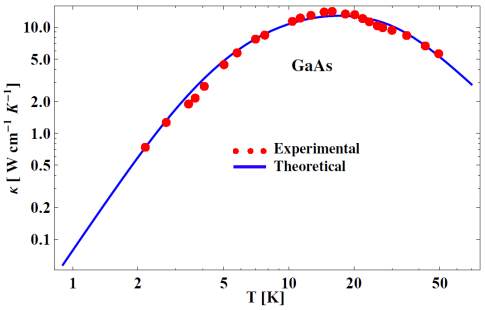

Fig. 10. Analysis of thermal conductivity of GaAs (sample III).

In order to examine present model, we have taken the experimental data of Holland [12] for the purpose of analysis of sample I, sample II, and sample III (three samples) in the temperature ranges (1.7–292.3), (1.7–170.3 K) and (2.1–49.3 K), respectively. The modified form of Eq. (1) is taken as

$$\kappa = \xi \int_0^{\omega_{\rm D}} \frac{\omega^4 \, {\rm e}^{\beta\hbar\omega} \, {\rm d}\omega}{[\tau_{\rm CB}^{-1} + \Gamma(\omega) + \tau_R^{-1}(\omega)]({\rm e}^{\beta\hbar\omega} - 1)^2}, \quad (35)$$

where

$$\xi = \frac{k_{\rm B}(\beta\hbar)^2}{2\pi^2 v}, \quad (36)$$

$$\Gamma(\omega) = \Gamma_k^{\rm D}(\omega) + \Gamma_k^{\rm 3A}(\omega) + \Gamma_k^{\rm AD}(\omega) + \Gamma_k^{\rm ep}(\omega). \quad (37)$$

The data used for the analysis are furnished in Table, the detailed explanation of them is given in Sect. 2. Due to the lack of availability of some data on anharmonic potentials and impurity concentration we had no option except taking A_1, A_2, B and D as adjustable parameters for the purpose of analysis of LTC of GaAs. This has been done by numerically integrating Eq. (35). However, these quantities can be exactly evaluated after collecting the sufficient information about effective anharmonic forces and impurity scenario which could not be made available in the present case and may be undertaken in future on the basis of the model presented in Sect. 2. It is observed

that at low temperatures, below the thermal conductivity maximum the major contribution to thermal conductivity comes from combined boundary scattering while the point defect scattering invokes at relatively elevated temperatures. The phonon–phonon and interference scattering processes dominate in the close vicinity of thermal conductivity maximum and above. The resonance scattering is also found effective in this region. Based on the new formulation the present calculations are depicted in Figs. 8, 9 and 10 which show an excellent agreement with experimental observations. The samples of GaAs have few impurities or crystal imperfections, i.e., a low number of electrically active impurities and no crystal faults are large enough to alter the thermal conductivity in the boundary scattering region. Hence need of any other scattering mechanism ceases.

4. Discussion and conclusions

The collision processes among phonons in the low temperature region (close to absolute zero) are very rare because a very small number of phonons with longer wavelengths get excited and scattered from crystal boundaries and microboundaries. Figure 1 exhibits high sensitivity of internal boundary parameter below 10 K. As the temperature starts rising the larger number of phonons with shorter wavelengths are excited and their free paths are limited by defects commencing the involvement of impurity scattering. The variation of impurity scattering contribution to thermal conductivity is depicted in Figs. 2 and 3. The contribution due to force constant changes of the form is $\approx A_2\omega^2$ which has never been included in any of the earlier studies. The importance of this term cannot be easily ignored because a very small change in central or noncentral force constants drastically changes the specific heat of a crystal. Let us note that the specific heat term appears in LTC expression;

$$\kappa = \frac{3}{(2\pi)^3}\int v^2\cos^2(\theta)\alpha(k)C_{\rm ph}(k)\,{\rm d}^3k.$$

Since the number of excited phonons continuously increases with gradually rising temperature towards LTC maximum, the probability of phonon–phonon scattering becomes comparable to defect scattering. The maximum of LTC appears when the mean free path for phonon–phonon scattering roughly becomes equivalent to that of impurity scattering which depends on the nature and number of defects in the crystal and the corresponding temperatures characteristic of the specimen rather than of chemical composition of the material [29]. Obviously, the possibility of interference scattering as shown in Fig. 4 takes the charge; i.e., phonons of impurity (localized) fields start interacting with the phonons of anharmonic phonon fields. It should be noted that the contribution from boundary scattering in this region starts losing its significance because of a huge number of phonons (with much shorter wavelengths and considerably small free paths comparable with interatomic spacing) and other scatterers which rarely allow the phonons to scatter from crystal boundaries. The resonance scattering is also found effective in this region (Fig. 7). The phonon–phonon and interference scattering processes appear as dominant scattering processes to offer sufficient thermal resistance in the close vicinity of thermal conductivity maximum and above. At the same time phonons from boundaries are rarely scattered and the impurity effects also start diminishing its influence. A three-dimensional graphics showing the variation of LTC with x and T is depicted as Fig. 11.

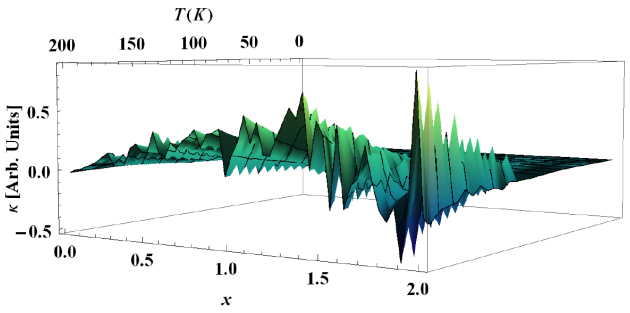

Fig. 11. LTC of GaAs (sample III) as a function of x and T.

This model entertains the effects of dispersion via $\Gamma_k(\omega)$ which really ascertains the frequency spectrum of a particular crystal including anharmonic effects and mass and force constant changes due to the impurity insertion. From present investigations based on the present model it emerges that the thermal conductivity of GaAs type crystals can be analyzed successfully and frequency line width concept is capable to repair several deficiencies left in earlier models. The objections and deficiencies occurring in the Callaway model have been removed with the help of this formulation and the theory is equally applicable to analyze the thermal conductivity data of other crystals and even that of high temperature superconductors [54].

Acknowledgments

One of the author (V.A.) is thankful to Ministry of Human Resource Development (MHRD) and Council of Scientific and Industrial Research (CSIR) Government of India, for providing the financial support to carry out this research work.

References

[1] R.J. Hardy, *J. Math. Phys.* **6**, 1749 (1965); *ibid.* **7**, 1435 (1966).

[2] K.R. Allen, J. Ford, *Phys. Rev.* **176**, 1046 (1968).

[3] P.G. Klemens, *Solid State Physics*, Vol. 7, Eds. F. Seitz, D. Turnbull, Academic Press, New York 1958, p. 1.

[4] P. Carruthers, *Rev. Mod. Phys.* **33**, 92 (1961).

[5] J.E. Parrott, A.D. Stukes, *Thermal Conductivity of Solids*, Pion Ltd., London 1975.

[6] R. Kubo, M. Yokota, S. Nakajima, *J. Phys. Soc. Jpn.* **12**, 1203 (1957).

[7] B.S. Semwal, P.K. Sharma, *J. Math. Phys.* **15**, 648 (1974).

[8] P.K. Sharma, Rita Bahadur, *Phys. Rev. B* **12**, 1522 (1975).

[9] J. Callaway, *Phys. Rev.* **113**, 1046 (1959).

[10] P. Erdos, S.B. Haley, *Phys. Rev.* **184**, 951 (1969).

[11] M.G. Holland, *Phys. Rev.* **132**, 2461 (1963).

[12] M.G. Holland, *Phys. Rev.* **134**, A471 (1963).

[13] P.G. Klemens, *Proc. R. Soc. (London) A* **68**, 1113 (1965).

[14] P.C. Sharma, K.S. Dubey, G.S. Verma, *Phys. Rev. B* **3**, 1985 (1971).

[15] M.D. Tiwari, K.B. Agrawal, *Phys. Rev. B* **4**, 3527 (1971).

[16] C.M. Bhandari, G.S. Verma, *Phys. Rev.* **138**, A2888 (1965); *ibid.* **140**, A2101 (1965).

[17] N.K.S. Gaur, C.M. Bhandari, G.S. Verma, *Physica* **32**, 1048 (1966).

[18] M.V. Klein, *Phys. Rev.* **141**, 716 (1966); *ibid.* **186**, 839 (1969).

[19] Anil Kumar, G.S. Verma, *Phys. Rev. B* **1**, 488 (1970).

[20] M.D. Tiwari, D.N. Talwar, K.B. Agrawal, *Solid State Commun.* **9**, 995 (1971).

[21] Anil Kumar, *Ind. J. Pure Appl. Phys.* **12**, 323 (1972); *ibid.* **15**, 300 (1977); *ibid.* **15**, 304 (1977); *Phys. Rev. B* **24**, 4493 (1981).

[22] G.P. Srivastava, *Philos. Mag.* **34**, 795 (1976); *J. Phys. (France)* **42**, C6:149 (1981); *ibid.* **42**, C6:253 (1981); *Physics of Phonons*, Adam Hilger, Bristol 1990.

[23] Y.P. Joshi, C.M. Bhandari, G.S. Verma, *Phys. Rev.* **83**, 3574 (1971).

[24] C.M. Bhandari, D.M. Rowe, *J. Phys. D, Appl. Phys.* **10**, L59 (1977); *J. Phys. C, Solid Phys.* **II**, 1787 (1979); *Prog. Cryst. Growth Charact.* **13**, 233 (1986).

[25] B. Saikia, Anil Kumar, *Pramana J. Phys.* **71**, 143 (2008).

[26] R.A.H. Hamilton, J.E. Parrott, *Phys. Rev.* **178**, 1284 (1969); *J. Phys. C, Solid State Phys.* **6**, 2653 (1973); *ibid.* **6**, 1863 (1973).

[27] J.E. Parrott, *J. Phys. C, Solid State Phys.* **15**, 6919 (1982).

[28] S. Adachi, *Physical Properties of III–V Semiconductor Compounds*, John Wiley & Sons, New York 1992; *J. Appl. Phys.* **54**, 1844 (1983).

[29] G. Grimvall, *Thermophysical Properties of Materials*, North-Holland, Amsterdam 1999, p. 255.

[30] V.I. Altukov, G.S. Zavt, *Phys. Status Solidi B* **64**, 403 (1974); *ibid.* **64**, 83 (1974).

[31] R.P. Gairola, *Acta Phys. Pol. A* **63**, 121 (1983).

[32] B.P. Bahuguna, C.P. Painuli, B.D. Indu, *Acta Phys. Pol. A* **80**, 527 (1991).

[33] D.A. Boriodo, M. Malorny, G. Bimer, N. Mingo, D.A. Stewart, *Appl. Phys. Lett.* **91**, 231922 (2009).

[34] L. Lindsay, D.A. Boriodo, *J. Phys., Condens. Matter* **20**, 165209 (2008).

[35] N. Mingo, D.A. Stewart, D.A. Boriodo, D. Srivastava, *Phys. Rev. B* **77**, 033418 (2008).

[36] A. Ward, D.A. Boriodo, *Phys. Rev. B* **77**, 245328 (2008).

[37] D. Feinburg, S. Ciouchi, F. de Pasquale, *Int. J. Mod. Phys. B* **1**, 1317 (1990).

[38] S.N. Behra, S.G. Mishra, *Phys. Rev. B* **31**, 2773 (1985).

[39] H.Y. Fan, *Elements of Solid State Physics*, Wiley, New York 1987.

[40] B.D. Indu, *Int. J. Mod. Phys. B* **4**, 1379 (1990).

[41] R.W.H. Stevenson, *Phonons in Perfect Lattice and Lattices with Point Imperfections*, Oliver and Boyd, London 1966.

[42] A.A. Maradudin, P.A. Flinn, R.A. Coldwell Horsefall, *Ann. Phys.* **15**, 337 (1961).

[43] H.B.G. Casimir, *Physica* **5**, 595 (1938).

[44] B.D. Indu, *Nuovo Cimento* **58B**, 345 (1980).

[45] B.D. Indu, *Mod. Phys. Lett. B* **6**, 1665 (1992).

[46] C. Herring, *Phys. Rev.* **95**, 954 (1954).

[47] M.G. Holland, L.J. Neuringer, in: *Proc. Int. Conf. Physics of Semiconductors, Exeter (UK)*, Inst. of Physics and the Physical Society, London 1962, p. 475.

[48] I. Pomeranchuk, *J. Phys. USSR* **4**, 259 (1941).

[49] I. Pomeranchuk, *J. Phys. USSR* **6**, 237 (1942).

[50] J.M. Ziman, *Philos. Mag.* **1**, 191 (1956).

[51] J.A. Carruthers, T.H. Geballe, H.M. Rosenberg, J.M. Ziman, *Proc. R. Soc. Lond. A* **238**, 995 (1957).

[52] A.P. Singh, A.Kr. Dimri, B.D. Indu, R.P. Vats, *Ind. J. Eng. Mater. Sci.* **8**, 219 (2001).

[53] M. Ataullah Ansari, N.P. Singh, B.D. Indu, *Ind. J. Pure Appl. Phys.* **45**, 27 (2007).

[54] Vinod Ashokan, B.D. Indu, *Thin Solid Films* **515**, e28 (2010); *Mod. Phys. Lett. B* **25**, 663 (2011).

[55] R.O. Pohl, *Phys. Rev. Lett.* **8**, 481 (1962).

[56] C.T. Walker, R.O. Pohl, *Phys. Rev.* **131**, 1433 (1963).

[57] V. Narayanamurti, W.D. Seward, R.O. Pohl, *Phys. Rev.* **148**, 481 (1966).

[58] M. Wagner, *Phys. Rev.* **122**, 450 (1961).

[59] J. Blakemore, *J. Appl. Phys.* **53**, R123 (1982).